

ON THE EXISTENCE AND STABILITY  
OF THREE-DIMENSIONAL SOLITONS AND VORTICES  
IN OPTICS AND BOSE-EINSTEIN CONDENSATE:  
OCCURRENCE OF SWALLOWTAIL BIFURCATIONS

D. MIHALACHE, D. MAZILU

*Horia Hulubei National Institute for Physics and Nuclear Engineering (IFIN-HH),  
Department of Theoretical Physics,  
407 Atomistilor, Magurele-Bucharest, 077125, Romania  
E-mail: Dumitru.Mihalache@nipne.ro*

(Received August 3, 2008)

*Abstract.* We give an overview of recent results in the area of three-dimensional nonspinning and spinning solitons in some selected models in optics and Bose-Einstein condensate (BEC). We concentrate on the existence and stability of these multiple dimensional localized structures and we reveal the occurrence of two cuspidal points in the Hamiltonian (BEC energy) versus soliton norm diagram, resulting in a generic swallowtail bifurcation.

*Key words:* spatiotemporal optical solitons, vortex solitons, Bose-Einstein condensate, swallowtail bifurcation.

## 1. INTRODUCTION

In the last years there has been an increasing interest in the theoretical and experimental study of shape-preserving confined structures of light, which overcome either temporal dispersion (the structure itself being localized in time), or spatial diffraction (the structure becomes localized in space) [1–4]. These multiple dimensional localized structures have attracted a great deal of attention both in optics and in the field of atomic Bose-Einstein condensate (BEC) [4]. In optics, these localized structures are quite complex physical objects, which are spatially confined on the order of wavelength (or even in the sub-wavelength scale). They represent the “particle-like” counterpart of the more common extended light structures. The optical medium that might sustain such confined self-guiding structures should be nonlinear, that is, its refractive index should be dependent on the light intensity. It has been shown during the last years that different types of nonlinearities of optical materials such as absorptive, dispersive, second-order (or

quadratic), third-order (or cubic, Kerr-like) can be used in practice to prevent either temporal dispersion or spatial diffraction of light beams or both of them. The field of optical solitons (either temporal or spatial ones) emerged from these fundamental studies of the interaction of intense laser beams with matter. This area is now in a mature stage; temporal optical solitons are now currently created in optical fibers and have led to a mature technology in photonics, whereas spatial optical solitons are currently created in various experimental conditions in laboratory and are now awaiting technological implementation.

However, there exist a third kind of optical solitons, which are spatially confined pulses of light, the so-called spatiotemporal optical solitons, alias “light bullets”, a term coined by Silberberg [5]. In the course of the past several years, a new level of understanding has been achieved about conditions for the existence, stability, and generation of spatiotemporal optical solitons, which are nondiffracting and nondispersing wavepackets propagating in nonlinear optical media. The spatiotemporal optical soliton is localized (self-guided) in the two transverse (spatial) dimensions and in the direction of propagation due to the balance of medium anomalous group-velocity dispersion (GVD) and nonlinear self-phase modulation. It is a fully three-dimensional (3D) localized object in both space and time. The term “light bullet” arises because it can be thought of as a tiny bead of light propagating long distances without changes (that is, nondispersing and nondiffracting in the propagating nonlinear medium). These localized physical objects could be used as information carriers in the all-optical processing information systems. It is believed that they are the ideal bits of information in both sequential (serial) and parallel transmission and processing information systems. Moreover, a useful scaling law exist that show that a smaller spatiotemporal soliton requires less energy. This field has been recently overviewed [4].

The solitons in media with the cubic self-focusing nonlinearity, obeying the nonlinear Schrödinger (NLS) equation, are unstable in two and three dimensions, because of the occurrence of collapse in the same model [6]. Several possibilities to arrest the collapse were considered, such as periodic alternation of self-focusing and defocusing layers [7] and various generalizations of this setting [8], and the use of weaker instabilities, *viz.*, saturable [9] or quadratic ( $\chi^{(2)}$ ) ones [10–13]. Tandem layered structures, composed of alternating linear and quadratic layers, were also proposed and investigated [14]. Other theoretically developed approaches use off-resonance two-level systems [15] and self-induced-transparency media [16].

Collapse does not occur either in cubic ( $\chi^{(3)}$ ) media whose nonlinearity is nonlocal [17, 18], therefore they may also give rise to stable solitons, see [19, 20]. Two-dimensional spatial solitons stabilized by the nonlocality were observed in vapors [21] and lead glasses featuring strong thermal nonlinearity [22]; in the latter case, elliptic and vortex-ring solitons were reported. Optical one-dimensional solitons supported by a nonlocal  $\chi^{(3)}$  nonlinearity were also created in liquid crystals [23]. Further, photonic lattices [24], vortices [25], spatial solitons in soft

matter [26], multiple vector solitons in nonlocal nonlinear media [27], and one-dimensional solitons of even and odd parities supported by competing nonlocal nonlinearities [28] were considered in the context of nonlocality. In addition, it was shown that long-range cubic nonlinearity induced by long-range interactions between atoms carrying polarized magnetic momenta in effectively two-dimensional Bose-Einstein condensates also leads to the prediction of stable two-dimensional (2D) solitons [29]. Moreover, 2D vortex solitons [25] and 3D fundamental and spinning solitons [30] were considered in the context of nonlocality in various models in optics and BEC.

The localized optical vortices (alias vortex solitons), have drawn much attention as objects of fundamental interest, and also due to their potential applications to all optical information processing, as well as to the guiding and trapping of atoms [31]. Unique properties are also featured by vortex clusters, such as rotation similar to the vortex motion in superfluids. The complex dynamics of vortex clusters in optical media with competing nonlinearities has been studied too [32]. Various complex patterns based on vortices were theoretically investigated in the usual BEC models, based on the Gross-Pitaevskii equation with the local nonlinearity [33]. However, it was found that, in the general case, multiple vortices nested in the host beam display strong instability, including distortion, drift and annihilation of the vortices.

Soliton necklaces [34–35] and rotating soliton clusters [36] were introduced, too. Moreover, in nondissipative optical media with competing nonlinearities, robust soliton complexes (in the form of “clusters” or soliton “molecules”) composed by several fundamental (nonspinning) solitons were thoroughly investigated, too [36]. It was found that the quasi-stable propagation of such soliton clusters is a generic feature of media with competing nonlinearities (self-focusing cubic and self-defocusing quintic nonlinearities or quadratic nonlinearities in competition with self-defocusing cubic nonlinearities).

Experimentally, only two-dimensional spatiotemporal solitons that overcome diffraction in one transverse spatial dimension have been created in quadratic nonlinear media [37]. However, there are no experiments yet concerning the creation of genuine 3D spatiotemporal solitons. Several groups all over the world are hunting for such physical objects with unique and useful properties from the technological point of view.

With regard to the theory, fundamentally new features of light pulses that self-trap in one or two transverse spatial dimensions and do not spread out in time, when propagating in various optical media, were thoroughly investigated in recent years in models with various nonlinearities. Both fundamental (nontopological) and topological (vorticity-carrying) stable 3D spatiotemporal solitons have been predicted, in media with competing optical nonlinearities (quadratic in competition with self-defocusing cubic or self-focusing cubic in competition with self-defocusing quintic) [38]. However, a very promising way to arrest the collapse in

Kerr-type focusing media is to use 2D nonlinear photonic lattices in a 3D environment. The study of coherent wave propagation in lattice systems [39–46], including soliton phenomena in nonlinear periodic structures, generated in recent years a lot of activity both in optics (for a recent comprehensive review, see [47]) and in the field of matter waves in optical trapping potentials [48].

The possibility of existence of stable three-dimensional spatiotemporal solitons confined by either harmonic two-dimensional optical lattices [49] or radially symmetric Bessel lattices [50] were investigated, too. We recently predicted the existence of stable three-dimensional spatiotemporal solitons in a two-dimensional photonic lattice; we found that the Hamiltonian-versus-soliton norm diagram exhibits a two-cusp structure. Correspondingly, a “swallowtail” shape of this diagram emerged, which is a quite rare physical phenomenon [49]. This unique feature is a generic one for both nontopological [49–52] and topological [53] 3D solitons: it has been also found in radially symmetric Bessel lattices [50] (a result suggesting a promising approach to generate stable “light bullets” in optics and stable 3D solitons in attractive Bose-Einstein condensates [51]), and in the search for stable 3D optical solitons in media with quadratic nonlinearities in competition with self-focusing cubic nonlinearities [52].

In the last years there is an increasing interest in the study of multidimensional dissipative localized structures which are modeled by nonlinear partial differential equations involving gain and loss terms in addition to the common nonlinear and dispersive/diffractive terms. These nonlinear dynamical systems allow for the formation under certain conditions of *stable dissipative solitons* [54]. One of the prototype dissipative dynamical system is that governed by the complex Ginzburg-Landau equation, which is one of the most studied nonlinear equations in the nonlinear science [55]. Recently stable fundamental (vorticityless) and spinning (with nonzero intrinsic vorticity) spatiotemporal dissipative optical solitons described by the complex cubic-quintic Ginzburg-Landau equation were found [56–63] and both elastic and inelastic collision scenarios were identified [64, 65].

In this work we briefly overview recent theoretical studies of the existence and stability of the families of 3D solitons and vortices in optics and BEC. The issue of existence and stability of multidimensional optical solitons in confining potentials is important in other relevant physical systems such as the investigation of Bose-Einstein condensates in periodic potentials created by laser standing waves.

We will concentrate on the existence and stability of these multiple dimensional localized structures and we will reveal the occurrence of two (or more) cuspidal points in the Hamiltonian (BEC energy) versus soliton norm diagram, resulting in a swallowtail bifurcation. We will consider the solitons trapped in both 2D [49] and 3D [51] Kerr-type harmonic photonic lattices and in cylindrical (radially symmetric) Bessel lattices [50] in self-focusing media. Moreover, we will

consider the fundamental (vorticityless) 3D solitons forming in media with quadratic and self-focusing cubic nonlinearities where such unique swallowtail bifurcation occurs, too [52]. The swallowtail bifurcation pattern occurs also in the case of 3D spinning solitons forming in low-dimensional (2D) harmonic lattices [53]. The issue of existence and stability of multidimensional solitons in confining potentials is of much importance in the field of BEC loaded in periodic potentials created by the interference of several laser standing waves.

## 2. STABLE 3D SOLITONS AND VORTICES SUPPORTED BY 2D OPTICAL LATTICES

The basic dimensionless evolution equation for 3D light propagation in a 2D photonic lattice is

$$i \frac{\partial q}{\partial \xi} = -\frac{1}{2} \left( \frac{\partial^2 q}{\partial \eta^2} + \frac{\partial^2 q}{\partial \zeta^2} \right) + \frac{d}{2} \frac{\partial^2 q}{\partial \tau^2} + \sigma q |q|^2 - p \cos(\Omega_\eta \eta) \cos(\Omega_\zeta \zeta) q. \quad (1)$$

Here we assume that the linear susceptibility depends on the transverse coordinates  $\eta$  and  $\zeta$ , that finally leads to the appearance of the linear term proportional to the modulation parameter  $p$ .  $\tau$  is the time coordinate and the parameter  $d$  equals the ratio of diffraction length to dispersion length. We consider  $d = -1$  because we can always rescale the time coordinate to get this value. The parameter  $\sigma$  defines the sign of the nonlinearity, and we consider the case of self-focusing nonlinearity ( $\sigma = -1$ ). The parameter  $p$  is proportional to the refractive index modulation depth. We take typical values in the interval  $0 < p < 20$ , and we have selected the transverse scale such that the modulation period is  $T = \pi/2$  [49].

Equation (1) conserves the energy

$$E = \iiint |q(\eta, \zeta, \tau)|^2 d\eta d\zeta d\tau \quad (2)$$

and the Hamiltonian  $H$  (see Ref. [49]).

We search for stationary soliton profiles in the form

$$q(\eta, \zeta, \tau, \xi) = w(\eta, \zeta, \tau) \exp(ib\xi), \quad (3)$$

where  $w$  is a real function and  $b$  is the nonlinear wave number shift. The resulting equation was solved by using the imaginary time propagation method. We have used a standard Crank-Nicholson finite difference scheme. The nonlinear finite-difference equations were solved by means of the Picard iteration method and the resulting linear system was handled with the help of the Gauss-Seidel iterative procedure. To achieve good convergence, we needed typically, six Picard iterations and six Gauss-Seidel iterations. We have employed equal transverse grid stepsizes

$h = \Delta\eta = \Delta\zeta = \Delta\tau$ . Typical values of the transverse stepsizes and longitudinal stepsizes are  $h = 0.008$  and  $\Delta\xi = 0.00006$  for high amplitude solitons. For low amplitude solitons we take typically  $h = 0.05$  and  $\Delta\xi = 0.002$ . We have used 401 points in each transverse direction and the stabilization process occurs after  $4 \times 10^3 - 1 \times 10^4$  steps along the propagation direction.

By a direct manipulation of the evolution equation (1) we get the following relationship between the total energy  $E$ , the wave number  $b$ , the stationary profile  $w$  and the Hamiltonian  $H$ :

$$H = -bE + \frac{1}{2} \iiint w^4 d\eta d\zeta d\tau. \quad (4)$$

This relationship may be used to determine the wave number  $b$ , once knowing the field profile  $w$ . Notice that for the stationary solitons of the 3D NLS equation (that is, the limit  $p = 0$  in Eq. (1)) the corresponding relationships between  $E$ ,  $H$ , and the wave number  $b$  are:

$$b(E) = CE^{-2}, \quad H(E) = CE^{-1}, \quad (5)$$

where  $C$  is a numerical constant:  $C \simeq 44.3$  (see, *e.g.*, [1, 2]). We mention that we have additionally cross-checked our imaginary time propagation code on the 3D NLS equation and we have tested the validity of the above relationships between the wave number  $b$ , the energy  $E$ , and the Hamiltonian  $H$ .

In Fig. 1 we plot the dependences  $b = b(E)$  (Fig. 1(a)) and  $H = H(E)$  (Fig. 1(b)) for the one-parameter family of 3D stationary solutions. We see that as a consequence of the imprinted 2D photonic lattice, the nonlinear localized states exist only for wave numbers  $b$  larger than some minimum values  $b_{min}(p)$  (the edge of the band-gap). This minimum propagation constant increases with the increase of the lattice strength parameter  $p$  (for the NLS equation we have  $b_{min} = 0$ ). Families of solitons exist whenever their energy exceeds a certain minimum value and are *linearly stable* in the intermediate-energy regime and for sufficiently high lattice potential (see the solid lines in Fig. 1 for lattice strengths  $p = 15$  and  $p = 20$ ). Remarkably, for sufficiently large values of the lattice strength parameter  $p$ , the Hamiltonian-versus-energy curves plotted in Fig. 1(b) display *two cusps*, instead of a single one as in other 2D and 3D Hamiltonian systems (see, *e.g.*, [2] for several examples of the usefulness of the Hamiltonian-versus-energy (norm) diagrams in the analysis of the existence and stability of solitons in conservative systems with an infinite number of degrees of freedom). This two-cusp structure of the Hamiltonian-soliton norm diagram is the so-called “swallowtail” catastrophe and is quite rare in physics (for a review on catastrophe theory as applied to the soliton stability see, *e.g.*, [66]).

We mention that only the soliton families which meet the Vakhitov-Kolokolov (VK) criterium  $dE/db > 0$  were expected to be linearly stable. However

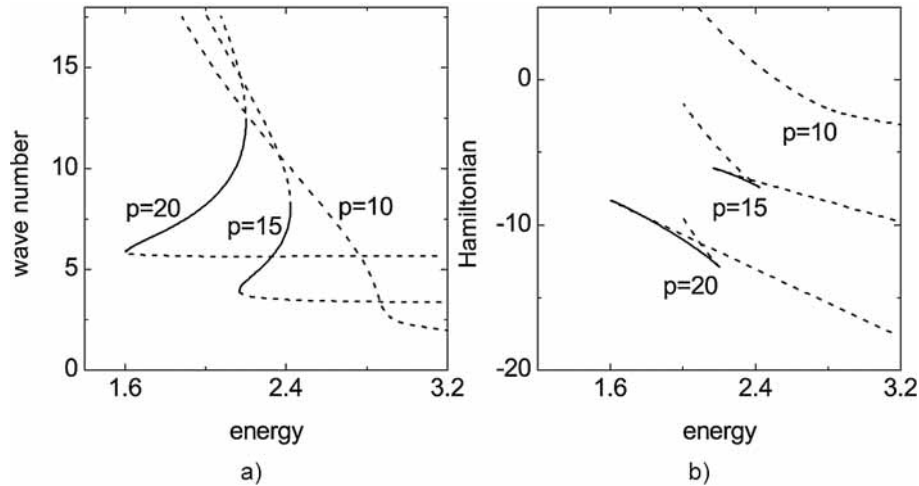


Fig. 1 – (a) The wave number  $b$  vs. energy (norm)  $E$ ; b) the Hamiltonian  $H$  vs. energy (norm)  $E$ . Solid and dashed lines depict stable and unstable soliton branches, respectively.

we have checked by direct propagation of perturbed stationary solitons that this is the case: the two semiinfinite branches corresponding to  $p = 15$  and  $p = 20$  [the dashed lines in Figs. 1(a,b)] correspond to unstable solitons, whereas the finite branches [the solid lines in Figs. 1(a,b)] correspond to stable 3D solitons. Thus we got stable 3D one-parameter soliton families if the lattice strength  $p$  exceeds some threshold value (see Figs. 1(a,b)).

Remarkably, this unique swallowtail bifurcation [66] occurs also in the study of the stability of spinning 3D solitons in the same model; see Fig. 2 for an example

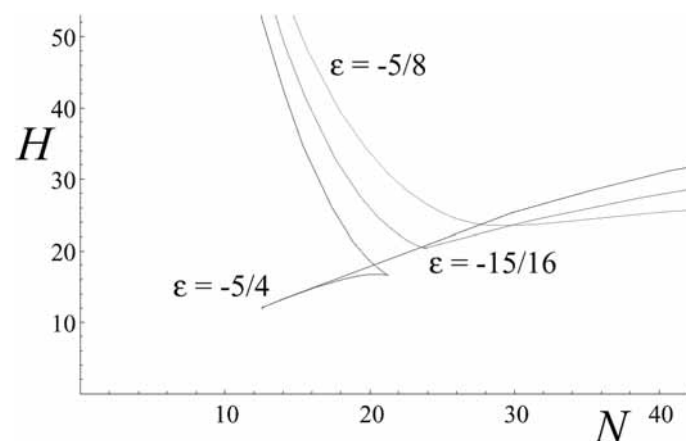


Fig. 2 – Dependences  $H = H(N)$  for the family of 3D solitons with  $S = 1$  (color online), as predicted by the variational approximation for several different values of strength  $\epsilon$  of the quasi-2D lattice.

example of two-cusp structure of the Hamiltonian- soliton norm diagram for the 3D solitons with vorticity  $S = 1$  supported by a 2D harmonic lattice if the lattice strength  $|\varepsilon|$  is large enough [53].

### 3. STABLE 3D OPTICAL SOLITONS SUPPORTED BY COMPETING QUADRATIC AND SELF-FOCUSING CUBIC-NONLINEARITIES

The general  $\chi^{(2)} : \chi^{(3)}$  model relevant for the 3D case was elaborated in Ref. [52]:

$$\begin{aligned} i \frac{\partial u}{\partial Z} + \frac{1}{2} \left( \frac{\partial^2 u}{\partial X^2} + \frac{\partial^2 u}{\partial Y^2} + \frac{\partial^2 u}{\partial T^2} \right) + u^* v + (|u|^2 + 2|v|^2)u &= 0, \\ i \frac{\partial v}{\partial Z} + \frac{1}{4} \left( \frac{\partial^2 v}{\partial X^2} + \frac{\partial^2 v}{\partial Y^2} + \sigma \frac{\partial^2 v}{\partial T^2} \right) - \beta v + u^2 + 2(2|u|^2 + |v|^2)v &= 0. \end{aligned} \quad (6)$$

Here,  $u$  and  $v$  are local amplitudes of the fundamental-frequency (FF) and second-harmonic (SH) waves with phase mismatch  $\beta$  between them,  $T$ ,  $(X, Y)$ , and  $Z$  are the reduced time, two transverse spatial coordinates, and propagation distance, and the  $\chi^{(2)}$  and  $\chi^{(3)}$  coefficients can be normalized as shown in the equations, without loss of generality. The above equations assume different GVD coefficients at the two harmonics, with ratio  $\sigma$  between them (the GVD coefficient in the equation for the FF component is normalized to be 1), but neglect the Poynting-vector misalignment between the waves, as well as the walkoff between them [12]. In the case of  $\sigma = 1$ , the model possesses an additional spatiotemporal spherical symmetry.

From dependences  $E = E(k)$  ( $E$  is the total energy and  $k$  is the nonlinear wave number) for the one-parameter family of stationary solitons, one can predict their stability on the basis of the VK criterion [6],  $dE/dk > 0$ , which is a necessary stability condition, securing the absence of instability eigenmodes with real eigenvalues in the spectrum of small perturbations around the solitons. In fact, for the fundamental solitons (on the contrary to their spinning counterparts) the VK criterion may be a sufficient stability condition also, as suggested, in particular, by the results presented below.

In Fig. 3, we display curves  $E = E(k)$  and  $H = H(E)$  for the one-parameter families of the soliton solutions. A noteworthy feature of these dependences is that the 3D solitons exist at exact phase matching ( $\beta = 0$ ) and at positive mismatch for any positive value of wave number  $k$ , whereas at negative  $\beta$  they exist only above a certain cutoff value, which is given by  $k_{co} = -\beta/2$ .

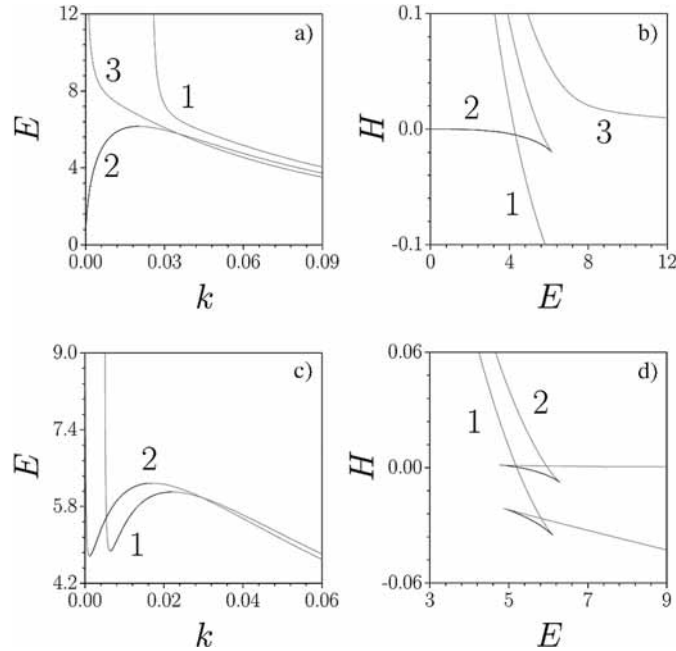


Fig. 3 – Characteristics of numerically found spatiotemporal soliton families for  $\sigma = 1$  (color online). (a), (c) Energy  $E$  vs. propagation constant  $k$ ; (b), (d): Hamiltonian vs.  $E$ . In panels (a) and (b), labels 1, 2 and 3 correspond to  $\beta = -0.05$ ,  $\beta = 0$ , and  $\beta = 0.05$ , respectively. In (c) and (d), labels 1 and 2 correspond to  $\beta = -0.01$  and  $\beta = 0.01$ . Red (dark grey) and black lines depict unstable and stable soliton branches, respectively.

We also observe that for  $\beta = 0$  and for moderate nonzero values of  $\beta$ , both positive or negative, the solitons are expected to be stable in certain intervals of wave numbers and energies, as they satisfy the VK criterion,  $dE/dk > 0$ . As said above, the criterion is a necessary (but, generally, not sufficient) stability condition for the soliton family. However, it was demonstrated by calculating the instability growth rates for small perturbations that the VK criterion is actually sufficient for the stability of the fundamental 3D solitons.

At exact phase-matching ( $\beta = 0$ ), the 3D solitons are stable for energies from zero up to a certain maximum value, and the Hamiltonian-*versus*-energy ( $H$ - $E$ ) diagram displays a single cuspidal point, whereas for moderate finite values of  $\beta$  (either positive or negative ones) the solitons are stable in intervals of energy between finite limits, and the respective  $H$ - $E$  diagrams feature a characteristic *swallowtail* shape, with two cuspidal points, instead of a single one as in typical 2D and 3D Hamiltonian systems.

### 4. 3D SOLITONS SUPPORTED BY RADIALLY SYMMETRIC BESSEL BEAMS

Next we briefly discuss the existence and stability of three-dimensional solitons supported by cylindrical Bessel lattices (BLs) in self-focusing media. We show numerically that the BLs support a family of 3D solitons, which are stable within one or *two* intervals of values of their norm, if the lattice strength exceeds a threshold value. In the latter case, the Hamiltonian-vs.-norm diagram has three cuspidal points (a “swallowtail” pattern). The model applies to Bose-Einstein condensates and to suitable optical media with saturable nonlinearity. Accordingly, the results suggest new potential ways of making stable 3D BEC solitons and “light bullets”.

We consider 3D solitons trapped in a BL, in the case of the cubic self-attraction [50]. This configuration can be directly implemented in BECs with a negative scattering length, illuminated by an optical Bessel beam. The corresponding normalized 3D Gross-Pitaevskii equation (GPE) for the wave function  $q$  is [50]:

$$i \frac{\partial q}{\partial \xi} = -\frac{1}{2} \left( \frac{\partial^2 q}{\partial \eta^2} + \frac{\partial^2 q}{\partial \zeta^2} \right) - \frac{1}{2} \frac{\partial^2 q}{\partial \tau^2} - |q|^2 q - \Pi(r)q, \quad (7)$$

where  $\xi$  is time,  $\tau$  and  $(\eta, \zeta)$  are, respectively, the coordinates along the beam and in the transverse plane, and  $r \equiv (\eta^2 + \zeta^2)^{1/2}$ . The effective potential  $-\Pi(r)$  is proportional to the local intensity of the red-detuned optical wave that traps atoms at its antinodes [being interested in self-supporting solitons in the BLs, we do not include a magnetic (parabolic) trapping potential]. We will concentrate on the case of  $\Pi(r) = pJ_0(\sqrt{2\beta}r)$ , with the Bessel function  $J_0$  generated by the diffraction-free cylindrical beam,  $p$  and  $\beta$  determining the strength and radial scale of the BL. Note that the effective potential created by the Bessel beam proper is proportional to  $-J_0^2$ , while the case of  $\Pi \sim J_0$  actually implies interference between the cylindrical beam and a stronger plane wave with an amplitude  $A_0$  at the same frequency (see Ref. [50]).

The numerical results for the existence and stability of the 3D solitons are summarized in Fig. 4 where we plot the Hamiltonian-energy (norm) diagram [50]. We found that the 3D solitons exist if the propagation constant  $b$  exceeds a certain minimum (cut-off) value  $b_{\text{co}}$ . The  $b_{\text{co}}$  increases with  $p$  [ $b_{\text{co}}(p)$  vanishes solely at  $p = 0$ , as the *unstable* free-space 3D solitons exist for all values of  $b$ ]. For the soliton family, the norm  $U$  is a non-monotonic function of the wave number  $b$ . According to the above-mentioned VK stability criterion, parts of the soliton family with  $dU/db > 0$  are stable against perturbations. This prediction was

confirmed by numerical calculation of the perturbation growth rates  $Re(\delta)$ , and it was shown that the soliton families are *completely stable* (against all perturbations) precisely in the regions singled out by the condition  $dU/db > 0$ . We have found that, for small values of the lattice strength  $p$ , the solitons are stable in a narrow interval of  $b$  to the right of the cut-off value  $b_{co}$ . However, solitons lose their stability for the propagation constants  $b$  exceeding a value at which  $dU/db = 0$ , in contrast to the BL-supported 2D solitons, that may be stable in their entire existence domain (in terms of  $b$ ) if the lattice strength  $p$  is large enough.

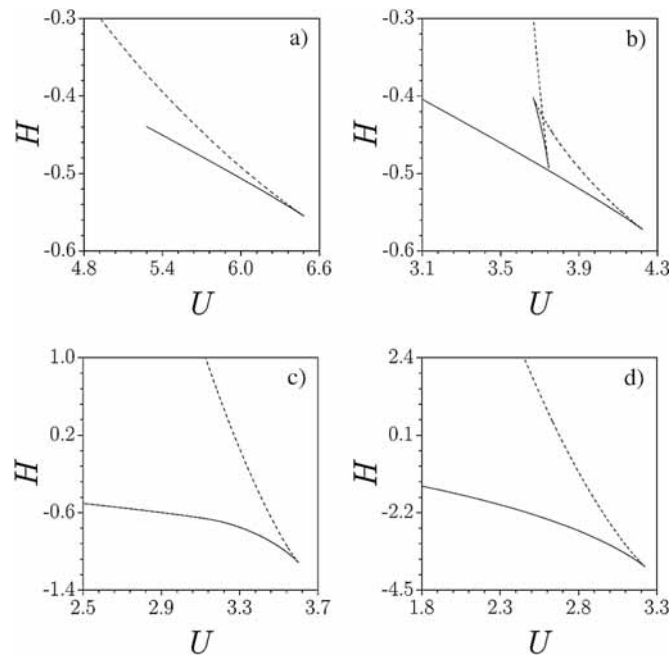


Fig. 4 – The Hamiltonian vs norm diagrams for  $p = 5$  (a), 5.5 (b), 6 (c), and 8 (d).

Remarkably, for some moderate values of  $p$ , the 3D solitons are stable in *two disjoint intervals* of  $b$  [one interval abuts on the cut-off value,  $b = b_{co}$ , and another one is found at relatively large values of the propagation constant, see Fig. 4(b)]. The Hamiltonian-energy (norm) diagram for the soliton families, which is a useful tool for the analysis of stability of solitons in conservative systems [2, 66], is plotted in Fig. 4 for several values of the lattice strength  $p$ . They exhibit one or, in some cases, three cuspidal points. In the latter case [see Fig. 4(b)] the diagram displays a “swallowtail” pattern, which actually accounts for the existence of two distinct stability regions for the 3D solitons. Although this pattern is one of generic possibilities known in the catastrophe theory, it occurs rather rarely in physical

models. A comprehensive review of applications of the catastrophe theory to the soliton-stability problem, based on the Whitney theorem for two-dimensional maps, which are constructed with the aid of the dynamical invariants of the nonlinear evolution equations, can be found in Ref. [66].

In Fig. 5 we display four typical examples of the stable 3D BL solitons. Low-amplitude broad (“loosely bound”) solitons extending over several radial-lattice rings, with the propagation constant  $b$  close to the cut-off  $b_{co}$ , are shown in Figs. 5(a, c), and high-amplitude (“tightly-bound”) ones, which are mostly trapped within the BL core, are presented in Figs. 5(b, d). We have additionally checked that the solitons which were predicted to be stable (see the solid-line segments in Fig. 4) were indeed stable in the direct simulations under input (white-noise) perturbations [50].

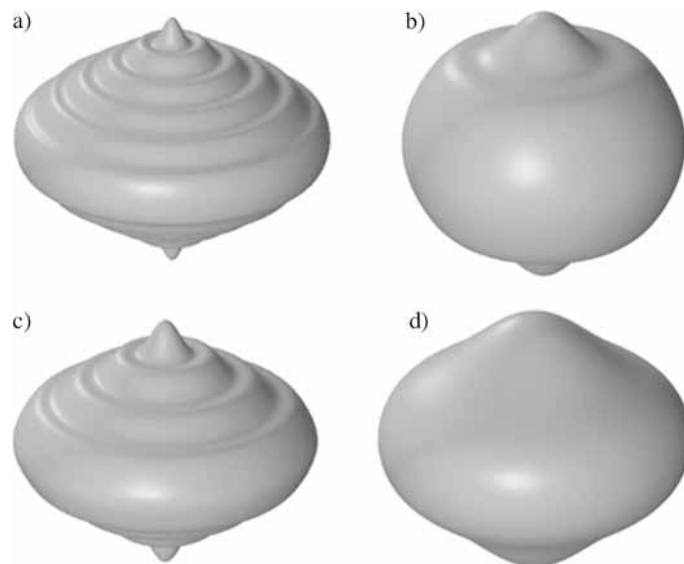


Fig. 5 – Isosurface plots for stationary stable solitons: (a)  $p = 5$ ,  $b = 0.11$ , and  $U = 6.477$ , (b)  $p = 5.5$ ,  $b = 0.85$ , and  $U = 3.677$ , (c)  $p = 6$ ,  $b = 0.23$ , and  $U = 2.623$ , and (d)  $p = 6$ ,  $b = 2$ , and  $U = 3.591$ .

## 5. 3D SOLITONS IN ATTRACTIVE BOSE-EINSTEIN CONDENSATES LOADED IN OPTICAL LATTICES

The creation of multidimensional solitons built of nonlinear light or matter waves is a great challenge to the experiment. The current situation in this field was summarized in a recent review [4]. A systematic investigation of the existence, stability and robustness of 3D BEC solitons in the 3D lattice potential has been

performed recently [51]. It is well known that the Gross-Pitaevski equation describes the BEC dynamics in terms of the mean-field single-atom wave function  $\psi(x, y, z, t)$ . The normalized form of this equation for a self-attractive condensate trapped in the 3D potential  $[-V(x, y, z)]$  is as follows [67–70]:

$$i\frac{\partial\psi}{\partial t} = -\frac{1}{2}\left(\frac{\partial^2\psi}{\partial x^2} + \frac{\partial^2\psi}{\partial y^2} + \frac{\partial^2\psi}{\partial z^2}\right) - |\psi|^2\psi - V(x, y, z)\psi. \quad (8)$$

Generally,  $V(x, y, z)$  contains terms accounting for the confining parabolic trap (magnetic and/or optical) and the periodic potential of the OL. Being interested in the localized solutions, occupying a few cells of the lattice, we disregard the parabolic potential and set  $V(x, y, z) = p[\cos(4x) + \cos(4y) + \cos(4z)]$ , where the OL period is normalized to be  $\pi/2$ , and the OL strength  $p$  is defined to be positive. Besides the norm,

$$N = \iiint |\psi(x, y, z)|^2 dx dy dz, \quad (9)$$

the above equation conserves the energy,

$$E = \iiint \left[ \frac{1}{2} \left( \left| \frac{\partial\psi}{\partial x} \right|^2 + \left| \frac{\partial\psi}{\partial y} \right|^2 + \left| \frac{\partial\psi}{\partial z} \right|^2 \right) - \frac{1}{2} |\psi|^4 - pV(x, y, z) |\psi|^2 \right] dx dy dz. \quad (10)$$

Stationary soliton solutions have the form  $\psi(x, y, z, t) = w(x, y, z) \cdot \exp(-i\mu t)$ , with a real function  $w$  and chemical potential  $\mu$ . We looked for the function  $w(x, y, z)$  by means of the known method of the propagation in imaginary time. It was implemented, using the Crank-Nicholson scheme, with the nonlinear finite-difference equations solved by means of the Picard iteration method, and the resulting linear system handled with the help of the Gauss-Seidel iterative procedure. To achieve good convergence, we typically needed six Picard iterations and six Gauss-Seidel iterations. We used equal transverse grid stepsizes,  $\Delta x = \Delta y = \Delta z \equiv h$ , and a mesh of  $361 \times 361 \times 361$  points was usually employed. The convergence to a stationary state occurred after  $4 \times 10^3$ – $5 \times 10^4$  steps of the evolution in imaginary time, typical transverse-grid and time stepsizes being  $h = 0.02$  and  $\Delta t = 0.0003$ , respectively, for narrow solitons, whereas for broad ones it was enough to take  $h = 0.07$  and  $\Delta t = 0.004$ .

One can derive a relationship between the norm  $N$ , chemical potential  $\mu$ , real wave function  $w$  and energy  $E$  of the stationary solution:

$$E = \mu N + \frac{1}{2} \iiint w^4(x, y, z) dx dy dz. \quad (11)$$

It can be used to determine the chemical potential  $\mu$ , once the field profile  $w$  is known. This exact relation was also used for verification of accuracy of the

numerically found stationary solutions. Notice that, for stationary solitons of the NLS equation in the free 3D space, the following relations between  $\mu$ ,  $N$ , and  $E$  is known:  $\mu(N) = -CN^{-2}$ ,  $E(N) = CN^{-1}$ ,  $C \approx 44.3$  [1, 2] (a corollary of this is  $d\mu/dN > 0$ , which immediately shows that these free-space solitons are *always unstable*, as the VK stability criterion requires exactly the opposite,  $d\mu/dN < 0$ ).

We have found that that, in the presence of the 3D OL, the localized states exist only for  $\mu$  smaller than some maximum value,  $\mu_{\max}(p)$ ; in fact, it corresponds to the edge of the *bandgap* in the spectrum of the linearized evolution equation. At values of  $\mu$  that do not belong to the bandgap, no soliton is possible. We note that  $\mu_{\max}(p)$  decreases with the increase of the lattice strength  $p$  [for the 3D NLS equation in free space ( $p = 0$ ), one has  $\mu_{\max}(0) = 0$ ]. Remarkably, for sufficiently large values of the lattice strength  $p$ , the  $E(N)$  curves feature *two cusps*, instead of a single one, as in most other 2D and 3D Hamiltonian models.

Further, Fig. 6 displays an integrated characteristic of the soliton family – the dependence  $E = E(\mu, N)$  – together with the corresponding projections onto the three planes  $(E, \mu)$ ,  $(E, N)$ , and  $(\mu, N)$ , for two different values of the lattice strength,  $p = 0$  and  $p = 3$ . In the latter case [in Fig. 6(b)], we notice the *non-monotonic* behavior of the three projected curves for  $p = 3$  (above the stability threshold) and the “*swallowtail*” loop in the energy-norm diagram.

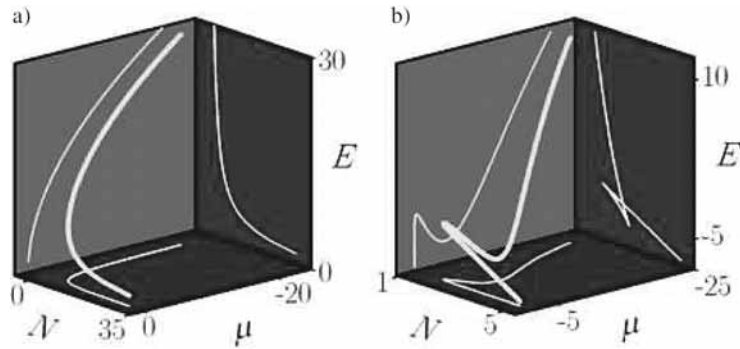


Fig. 6 – The soliton family in terms (color online) of the dependence  $E = E(\mu, N)$ , and its projections on the planes  $(E, \mu)$ ,  $(E, N)$ , and  $(\mu, N)$  for  $p = 0$  (a) and  $p = 3$  (b).

Shapes of both unstable and stable solitons are shown in Fig. 7, through their isosurface plots for a typical value of the lattice strength parameter,  $p = 3$ . An unstable low-amplitude 3D soliton (with  $A \equiv w(0, 0, 0) = 1.8$ ), found for the value of the chemical potential  $\mu$  close to the bandgap edge, is displayed in Fig. 7(a). This soliton is broad, occupying many lattice cells. Typical *stable* solitons, with medium ( $A = 2.2$ ) and high ( $A = 3$ ) amplitude, are shown in Figs. 7(b) and Fig. 7(c), respectively. Notice that the unstable soliton in Fig. 7(a) and its stable

counterpart in Fig. 7(c) have *equal values of the norm*,  $N = 2.4$ . The intermediate stable soliton in Fig. 7(b) has a smaller norm ( $N = 2.04$ ), which is very close to the limit value corresponding to the first cuspidal point in the dependence  $E = E(N)$ . Fig. 8 additionally shows integrated views along the  $z$ -axis of the isosurface plots displayed in Fig. 7. This figure illustrates the fact that low-amplitude solitons spread to many lattice cells, whereas high-amplitude solitons occupy only a few cells.

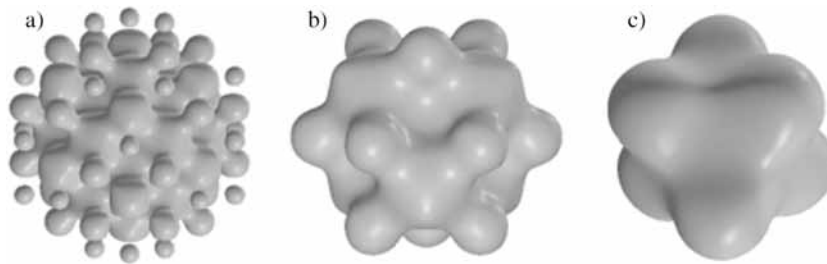


Fig. 7 – Isosurface plots of unstable (a) and stable (b) and (c) 3D solitons. Here  $p = 3$ ;  
a)  $N = 2.4$ ,  $A = 1.8$ ; b)  $N = 2.04$ ,  $A = 2.2$ ; c)  $N = 2.4$ ,  $A = 3$ .

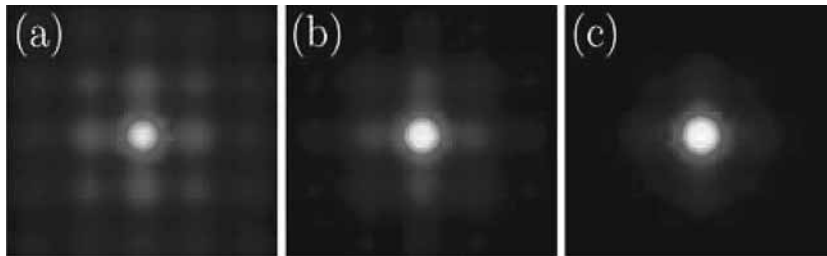


Fig. 8 – Integrated through views along the  $z$ -axis (color online) of the solitons shown in Fig. 7.

To illustrate the stability analysis, Fig. 9 shows an example of a stable soliton which persists after the application of the stochastic perturbation: in the course of the evolution, the soliton's amplitude slightly oscillates, with no trend to collapse or breakup. For linearly unstable solitons, the simulations reveal the following scenarios of the instability development: (i) low-amplitude solitons decay into linear waves under stochastic perturbations, or under uniform ones that reduce the soliton's norm; this case is illustrated by Fig. 10 for a typical situation, (ii) the same unstable soliton, but under uniform perturbations (that make its norm larger), reshapes itself into a time-periodic breather, and (iii) an unstable high-amplitude soliton collapses if it is perturbed by the uniform perturbation that increases its norm [51].

Notice also that a repulsive BEC confined in a 3D optical lattice supports spatially localized (in all three dimensions) vortex structures which are remarkably robust and which possess highly nontrivial particle flows [71].

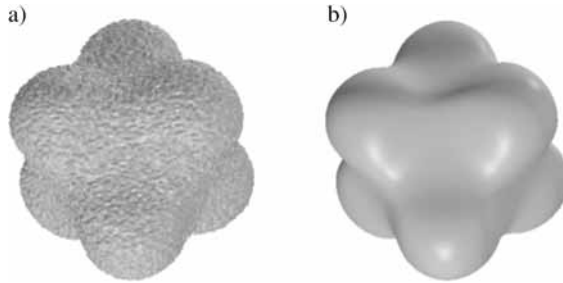


Fig. 9 – Isosurface plots showing self-cleaning of a stable soliton corresponding to  $p = 3$  and  $N = 2.4$ , initially perturbed by white noise. (a) Input at  $t = 0$ ; (b) output at  $t = 50$ .

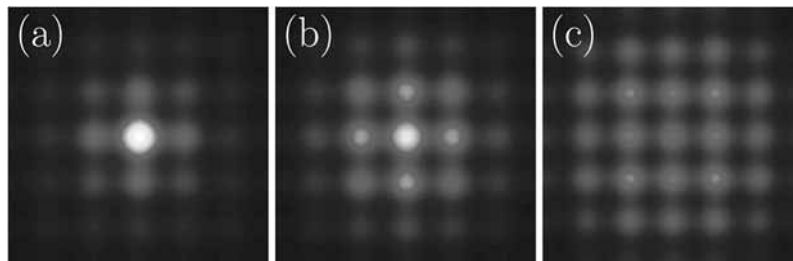


Fig. 10 – Integrated through views along (color online) the  $z$ -axis of an unstable soliton that decays due to a uniform norm-reducing perturbation with  $\epsilon = 0.01$ , for  $p = 3$ : a)  $t = 0$ ,  $A = 1.78$ ; b)  $t = 50$ ,  $A = 0.6505$ , c)  $t = 70$ ,  $A = 0.2075$ .

## 6. CONCLUSIONS

In this work we overviewed some recent results concerning the existence, stability and robustness of three-dimensional solitons and vortices in selected models in optics and Bose-Einstein condensate. We have shown that the Hamiltonian-versus-soliton norm curves are very useful in the analysis of existence and stability of solitons [2, 72]. We revealed the occurrence of a generic swallowtail bifurcation in the Hamiltonian-versus-soliton norm diagrams. The swallowtail-like bifurcation pattern, which actually accounts for the existence of two distinct stability regions for the three-dimensional fundamental (nonspinning) and spinning solitons is one of generic possibilities known in the catastrophe theory. However, it occurs rather rarely in the study of realistic physical models.

*Acknowledgements.* Part of the research work overviewed in this paper has been carried out in collaboration with Lucian-Cornel Crasovan, Yaroslav V. Kartashov, Yuri S. Kivshar, Hervé Leblond, Falk Lederer, Boris A. Malomed, and Lluís Torner. We are deeply indebted to all of them.

## REFERENCES

1. Y. S. Kivshar, G. P. Agrawal, *Optical solitons: From fibers to photonic crystals*, Academic Press, San Diego, 2003.

2. N. N. Akhmediev, A. Ankiewicz, *Solitons: Nonlinear Pulses and Beams*, London, Chapman and Hall, 1997.
3. G. I. Stegeman, D. N. Christodoulides, M. Segev, *IEEE J. Select. Top. Quant. Electron.*, **6**, 1419 (2000).
4. B. A. Malomed, D. Mihalache, F. Wise, L. Torner, *J. Opt. B: Quantum Semiclassical Opt.*, **7**, R53 (2005).
5. Y. Silberberg, *Opt. Lett.*, **15**, 1282 (1990).
6. L. Bergé, *Phys. Rep.*, **303**, 260 (1998); V. V. Konotop, P. Pacciani, *Phys. Rev. Lett.*, **94**, 240405 (2005).
7. I. Towers, B. A. Malomed, *J. Opt. Soc. Am.*, **19**, 537 (2002).
8. B. A. Malomed, *Soliton Management in Periodic Systems*, Springer, New York, 2006.
9. D. Edmundson, R. H. Enns, *Opt. Lett.*, **17**, 586 (1992); N. Akhmediev, J. M. Soto-Crespo, *Phys. Rev.*, A **47**, 1358 (1993); R. McLeod, K. Wagner, S. Blair, *Phys. Rev.*, A **52**, 3254 (1995).
10. B. A. Malomed *et al.*, *Phys. Rev.*, E **56**, 4725 (1997).
11. D. V. Skryabin, W. J. Firth, *Opt. Commun.*, **148**, 79 (1998).
12. L. Torner, D. Mazilu, D. Mihalache, *Phys. Rev. Lett.*, **77**, 2455 (1996); D. Mihalache, F. Lederer, D. Mazilu, L. C. Crasovan, *Opt. Eng.*, **35**, 1616 (1996); D. Mihalache, D. Mazilu, L. C. Crasovan, L. Torner, *Opt. Commun.*, **137**, 113 (1997); D. Mihalache *et al.*, *Phys. Rev.*, E **62**, R1505 (2000).
13. D. Mihalache *et al.*, *Opt. Commun.*, **152**, 365 (1998); *Opt. Commun.*, **169**, 341 (1999); *Opt. Commun.*, **159**, 129 (1999); *Phys. Rev.*, E **62**, 7340 (2000); N. C. Panoiu *et al.*, *Phys. Rev.*, E **71**, 036615 (2005).
14. L. Torner *et al.*, *Opt. Commun.*, **199**, 277 (2001).
15. I. V. Mel'nikov, D. Mihalache, N. C. Panoiu, *Opt. Commun.*, **181**, 345 (2000).
16. M. Blaauboer, B. A. Malomed, G. Kurizki, *Phys. Rev. Lett.*, **84**, 1906 (2000).
17. S. K. Turitsyn, *Theor. Math. Phys.*, **64**, 797 (1985).
18. W. Krolikowski, O. Bang, *Phys. Rev.*, E **63**, 016610 (2001); M. Peccianti, C. Conti, G. Assanto, *Phys. Rev.*, E **68**, 025602 (2003).
19. W. Krolikowski *et al.*, *J. Opt. B: Quantum Semiclass. Opt.*, **6**, S288 (2004).
20. D. Mihalache, *Rom. Rep. Phys.*, **59**, 515 (2007).
21. D. Suter T. Blasberg, *Phys. Rev.*, A **48**, 4583 (1993).
22. C. Rotschild, O. Cohen, O. Manela, M. Segev, T. Carmon, *Phys. Rev. Lett.*, **95**, 213904 (2005).
23. X. Hutsebaut *et al.*, *Opt. Commun.*, **233**, 217 (2004); C. Conti, M. Peccianti, G. Assanto, *Phys. Rev. Lett.*, **92**, 113902 (2004).
24. Y. V. Kartashov, V. A. Vysloukh, L. Torner, *Phys. Rev. Lett.*, **93**, 153903 (2004); Z. Xu, Y. V. Kartashov, L. Torner, *Phys. Rev. Lett.*, **95**, 113901 (2005); A. S. Desyatnikov *et al.*, *Opt. Lett.*, **30**, 869 (2005).
25. D. Briedis *et al.*, *Opt. Express*, **13**, 435 (2005); A. I. Yakimenko, Y. A. Zaliznyak, Y. Kivshar, *Phys. Rev.*, E **71**, 065603 (2005); A. I. Yakimenko, V. M. Lashkin, O. O. Prikhodko, *Phys. Rev.*, E **73**, 066605 (2006); V. M. Lashkin, *Phys. Rev.*, A **75**, 043607 (2007).
26. C. Conti, G. Ruocco, S. Trillo, *Phys. Rev. Lett.*, **95**, 183902 (2005).
27. Y. V. Kartashov, L. Torner, V. A. Vysloukh, D. Mihalache, *Opt. Lett.*, **31**, 1483 (2006).
28. D. Mihalache *et al.*, *Phys. Rev.*, E **74**, 066614 (2006).
29. P. Pedri, L. Santos, *Phys. Rev. Lett.*, **95**, 200404 (2005).
30. D. Mihalache *et al.*, *Phys. Rev.*, E **73**, 025601 (2006); Yu. A. Zaliznyak, A. I. Yakimenko, *Phys. Lett.*, A **372**, 2862 (2008).
31. D. Rozas, Z. S. Sacks, G. A. Swartzlander, *Phys. Rev. Lett.*, **79**, 3399 (1997).
32. D. Mihalache *et al.*, *Phys. Rev.*, E **67**, 055603 (2003); D. Mihalache *et al.*, *J. Opt. B: Quantum Semiclassical Opt.*, **6**, S341 (2004); M. J. Paz-Alonso, H. Michinel, *Phys. Rev. Lett.*, **94**, 093901 (2005).

33. L. C. Crasovan *et al.*, Phys. Rev., E **66**, 036612 (2002); L. C. Crasovan *et al.*, Phys. Rev., A **68**, 063609 (2003); T. Mizushima, N. Kobayashi, K. Machida, Phys. Rev., A **70**, 043613 (2004); M. Mottonen, S. M. M. Virtanen, T. Isoshima, M. M. Salomaa, Phys. Rev., A **71**, 033626 (2005).
34. M. Soljacic, S. Sears, M. Segev, Phys. Rev. Lett., **81**, 4851 (1998); A. S. Desyatnikov Y. S. Kivshar, Phys. Rev. Lett., **87**, 033901 (2001).
35. Y. J. He, H. H. Fan, J. W. Dong, H. Z. Wang, Phys. Rev., E **74**, 016611 (2006); Y. J. He, B. A. Malomed, H. Z. Wang, Opt. Express, **15**, 17502 (2007); Y. J. He, B. A. Malomed, D. Mihalache, H. Z. Wang, Phys. Rev., A **77**, 043826 (2008).
36. A. S. Desyatnikov Y. S. Kivshar, Phys. Rev. Lett., **88**, 053901 (2002); Y. V. Kartashov *et al.*, Phys. Rev. Lett., **89**, 273902 (2002); L. C. Crasovan *et al.*, Phys. Rev., E **67**, 046610 (2003); D. Mihalache *et al.*, Phys. Rev., E **68**, 046612 (2003); D. Mihalache *et al.*, J. Opt. B: Quantum Semiclassical Opt., **6**, S333 (2004).
37. X. Liu, L. J. Qian, F. W. Wise, Phys. Rev. Lett., **82**, 4631 (1999).
38. D. Mihalache *et al.*, Phys. Rev. Lett., **88**, 073902 (2002); D. Mihalache *et al.*, Phys. Rev., E **66**, 016613 (2002); H. Michinel, M. J. Paz-Alonso, V. M. Perez-Garcia, Phys. Rev. Lett., **96**, 023903 (2006).
39. J. W. Fleischer, M. Segev, N. K. Efremidis, D. N. Christodoulides, Nature, **422**, 147 (2003); J. W. Fleischer, T. Carmon, M. Segev, N. K. Efremidis, D. N. Christodoulides, Phys. Rev. Lett., **90**, 023902 (2003).
40. D. Neshev, E. Ostrovskaya, Y. Kivshar, W. Krolikowski, Opt. Lett., **28**, 710 (2003); D. Neshev *et al.*, Phys. Rev. Lett., **92**, 123903 (2004).
41. N. K. Efremidis, S. Sears, D. N. Christodoulides, J. W. Fleischer, M. Segev, Phys. Rev., E **66**, 046602 (2002); N. K. Efremidis, J. Hudock, D. N. Christodoulides, J. W. Fleischer, O. Cohen, M. Segev, Phys. Rev. Lett., **91**, 213906 (2003).
42. Z. Chen *et al.*, Phys. Rev. Lett., **92**, 143902 (2004).
43. B. B. Baizakov, B. A. Malomed, M. Salerno, Europhys. Lett., **63**, 642 (2003); G. L. Alfimov, V. V. Konotop, M. Salerno, Europhys. Lett., **58**, 7 (2002).
44. Y. V. Kartashov *et al.*, Opt. Lett., **29**, 766 (2004).
45. Y. V. Kartashov, L. Torner, V. A. Vysloukh, Opt. Lett., **29**, 1102 (2004).
46. J. Yang, Z. H. Musslimani, Opt. Lett., **28**, 2094 (2003); Z. H. Musslimani, J. Yang, J. Opt. Soc. Am., B **21**, 973 (2004).
47. D. N. Christodoulides, F. Lederer, Y. Silberberg, Nature, **424**, 817 (2003).
48. B. P. Anderson, M. Kasevich, Science, **282**, 1686 (1998).
49. D. Mihalache *et al.*, Phys. Rev., E **70**, 055603 (2004).
50. D. Mihalache *et al.*, Phys. Rev. Lett., **95**, 023902 (2005).
51. D. Mihalache *et al.*, Phys. Rev., A **72**, 021601 (2005).
52. D. Mihalache *et al.*, Phys. Rev., E, 047601 (2006).
53. H. Leblond, B. A. Malomed, D. Mihalache Phys. Rev., E **76**, 026604 (2007).
54. N. Akhmediev, A. Ankiewicz (Eds.), *Dissipative Solitons*, Lect. Notes Phys., **661**, Springer, Berlin, 2005.
55. I. S. Aranson, L. Kramer, Rev. Mod. Phys., **74**, 99 (2002); P. Mandel, M. Tlidi, J. Opt. B: Quantum Semiclass. Opt., **6**, R60 (2004); B. A. Malomed, in *Encyclopedia of Nonlinear Science*, p. 157. A. Scott (Ed.), Routledge, New York, 2005.
56. L. C. Crasovan, B. A. Malomed, D. Mihalache, Phys. Rev., E **63**, 016605 (2001); L. C. Crasovan, B. A. Malomed, D. Mihalache, Phys. Lett., A **289**, 59 (2001).
57. D. Mihalache *et al.*, Phys. Rev. Lett., **97**, 073904 (2006).
58. D. Mihalache, D. Mazilu, F. Lederer, H. Leblond, B. A. Malomed, Phys. Rev., A **75**, 033811 (2007); D. Mihalache *et al.*, Phys. Rev., A **76**, 045803 (2007).
59. D. Mihalache, D. Mazilu, F. Lederer, Y. S. Kivshar, Phys. Rev., A **77**, 043828 (2008).

60. P. Grelu, J. M. Soto-Crespo, N. Akhmediev, *Opt. Express*, **13**, 9352 (2005); J. M. Soto-Crespo, P. Grelu, N. Akhmediev, *Opt. Express*, **14**, 4013 (2006).
61. V. Skarka, N. B. Aleksić, *Phys. Rev. Lett.* **96**, 013903 (2006).
62. J. M. Soto-Crespo, N. Akhmediev, P. Grelu, *Phys. Rev., E* **74**, 046612 (2006); N. Akhmediev, J. M. Soto-Crespo, P. Grelu, *Chaos*, **17**, 037112 (2007).
63. D. Mihalache, *Cent. Eur. J. Phys.*, **6**, 582 (2008); D. Mihalache, D. Mazilu, *Rom. Rep. Phys.*, **60**, 749 (2008).
64. D. Mihalache, D. Mazilu, F. Lederer, H. Leblond, B. A. Malomed, *Phys. Rev., A* **77**, 033817 (2008).
65. Y. Hong, T. Yi, *Chin. Phys., B* **17**, 1008 (2008).
66. F. V. Kusmartsev, *Phys. Rep.*, **183**, 1 (1989).
67. E. P. Gross, *Nuovo Cimento*, **20**, 454 (1961); L. P. Pitaevskii, *Sov. Phys. JETP*, **13**, 451 (1961).
68. F. Dalfovo *et al.*, *Rev. Mod. Phys.*, **71**, 463 (1999).
69. V. A. Brazhnyi V. V. Konotop, *Mod. Phys. Lett., B* **18**, 627 (2004); F. Kh. Abdullaev, A. Gammal, A. M. Kamchatnov, L. Tomio, *Int. J. Mod. Phys., B* **19**, 3415 (2005).
70. D. Mihalache *et al.*, *Phys. Rev., A* **73**, 043615 (2006); B. A. Malomed *et al.*, *Phys. Lett., A* **361**, 336 (2007).
71. T. J. Alexander, E. A. Ostrovskaya, A. A. Sukhorukov, Y. S. Kivshar, *Phys. Rev., A* **72**, 043603 (2005).
72. A. Ankiewicz, N. Akhmediev, *IEE Proc.-Optoelectron.*, **150**, 519 (2003).